Journal of Applied Electrochemistry **34**: 61–66, 2004.

Preparation of Pt–Ru bimetallic anodes by galvanostatic pulse electrodeposition: characterization and application to the direct methanol fuel cell

C. COUTANCEAU*, A.F. RAKOTONDRAINIBÉ, A. LIMA, E. GARNIER, S. PRONIER, J-M. LÉGER and C. LAMY

Equipe Electrocatalyse, UMR CNRS 6503, Université de Poitiers, 40, avenue du Recteur Pineau, 86022 Poitiers, France

*(*author for correspondence, e-mail: christophe.coutanceau@univ-poitiers.fr)*

Received 25 November 2002; accepted in revised form 24 June 2003

Key words: carbon electrode, DMFC, electrodeposition, galvanostatic pulses, platinum–ruthenium catalysts

Abstract

The electrodeposition of platinum and ruthenium was carried out on carbon electrodes to prepare methanol anodes with different Pt/Ru atomic ratios using a galvanostatic pulse technique. Characterizations by XRD, TEM, EDX and atomic absorption spectroscopy indicated that most of the electrocatalytic anodes consisted of 2 mg cm^{-2} of Pt–Ru alloy particles with the desired composition and with particle sizes ranging from 5 to 8 nm. Electrochemical tests in a single DMFC show that these electrodes are very active for methanol oxidation and that the best Pt/Ru atomic ratio in the temperature range used (50–110 °C) is 80:20. The influence of the relaxation time t_{off} was also studied and it appeared that a low t_{off} led to smaller particle sizes and higher performances in terms of current density and power density.

1. Introduction

The main challenge for the development of DMFCs is to reduce the noble metal catalyst loading of the electrodes and the associated cost without decreasing the efficiency of the fuel cell [1–3]. To achieve this goal, it is necessary to increase the effective surface area of the catalysts, that is, to increase the surface contact between the catalyst, the electronic conductor (carbon), the electrolyte (Nafion®) and the reactant (methanol). The electrochemical reaction occurs in this active part of the electrodes and thus the performances depend greatly on the kinetics of interfacial phenomena [4, 5].

Usually, electrodes for PEMFCs (polymer exchange membrane fuel cells) are constituted of black carbon powder which acts as a catalyst support and solid electrolyte such as Nafion® [6–10]. In this case, to increase the performance of the electrodes (i.e., the true surface area of the catalyst) one needs either to increase the thickness of the active layer, for a given catalyst loading, or to increase the amount of catalyst in the catalytic powder. Increasing the thickness of the active layer leads to a decrease in the diffusion rate of the reactant towards the catalytic sites, whereas increasing the weight loading generally leads to an increase in the particle size of the catalysts, thus decreasing their efficiency. Moreover, the most used methods of preparation of carbon supported catalysts by the colloidal route, necessitate heating or oxidative treatment in order to clean the catalyst particles from surfactant contamination [11, 12]. These treatments can greatly alter the surface structure of the particles [13].

One way to avoid these problems is to prepare electrodes by electrodeposition of metals at carbon electrodes. In a previous paper [14], we have shown that it is possible to deposit platinum, ruthenium and molybdenum at carbon electrodes in a reproducible way by applying a constant potential. It has also been shown that these anodes could be used in DMFCs. Since it is generally recognized that Pt/Ru alloys are the most active catalysts for the oxidation of methanol [5–18], this paper deals with the preparation, characterization and fuel cell tests of Pt–Ru anodes of different atomic composition prepared by galvanostatic pulse electrodeposition on a carbon support.

Some papers concern the electrodeposition of bimetallic systems by galvanostatic pulses [19] but, to our knowledge, none deals with Pt–Ru deposition. However, some authors have described the electrochemical deposition, at constant potential, of bimetallic Pt–Ru catalysts [14, 20]. Some articles describing the electrodeposition of platinum on a carbon support are available [3, 21–25]. Gloaguen et al. [26] and Thomson et al. [27] have studied effective cathodes for hydrogen/oxygen fuel cells prepared by potentiostatic pulse electrodeposition of platinum on carbon electrodes, whereas Choi et al. [28] used galvanostatic pulse electrodeposition. The galvanostatic technique is more convenient to

prepare high geometric surface area electrodes, because the electrical set up requires only two electrodes and an arbitrary waveform generator, whereas the potentiostatic set up requires a three electrode configuration. The potentiostatic technique is not convenient for electrodes with large geometric surface area (greater than about 10 cm^2).

The main goal of this work is to show that Pt–Ru bimetallic anodes can be prepared reproducibly using the technique of metal electrodeposition by galvanostatic pulses and that these anodes display good performance in a DMFC.

2. Experimental details

All solutions were prepared using Alfa Aesar® salts of platinum (K_2PtCl_6) and ruthenium (K_2RuCl_5) dissolved in 1.0 M H_2SO_4 (suprapur from Merck) in ultrapure water (MilliQ Millipore). Carbon gas diffusion electrodes of 10 cm^2 geometric surface area were made using a carbon cloth from Electrochem Inc. on which an ink made of Vulcan XC72 carbon powder and PTFE dissolved in isopropanol was painted. The gas diffusion electrodes were loaded with a 4 mg cm^{-2} mixture of carbon powder and 15 wt.% PTFE. The galvanostatic pulse deposition of platinum and ruthenium was carried out in a two electrode cell using a high power potentiostat (Wenking model HP 88) and an arbitrary waveform generator (Hewlett Packard 33120A). The pulse programs were processed by a home made software. Figure 1 shows the scheme of the electrical set-up. The output current applied between the two electrodes was monitored using a Tektronix digital storage oscilloscope. The time program for the current pulses was 0.1 s (t_{on}) at $j = 20$ mA cm^{-2}, and 2.5 s or 0.3 s (t_{off}) of relaxation time at $j = 0$. To avoid the formation of ruthenium oxides at the counter electrode, a pretreated Nafion® 112 membrane was inserted between the deposition compartment containing the solution of metallic salts in 1.0 M H_2SO_4 and the counter electrode compartment containing only 1.0 M H_2SO_4. After deposition of the metals, the electrodes were thoroughly rinsed with ultrapure water.

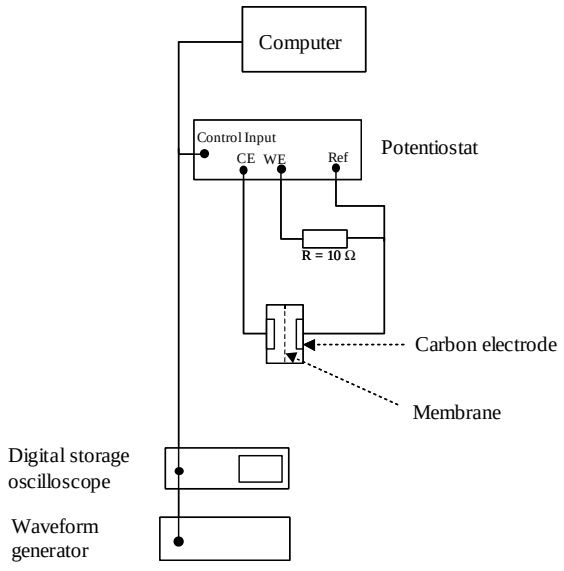

Fig. 1. Scheme of the electrical set-up used for the galvanostatic pulse electrodeposition.

Prior to the preparation of the membrane electrode assembly (MEA), a mixture of water and 5 wt. % Nafion® in alcohol was spread on the electrode surface, which was then dried at 90 °C in an oven and heated at 150 °C to recast the Nafion® film. The Nafion® loading of the electrode was 0.8 mg cm^{-2}. The MEAs were prepared by hot pressing (130 °C, 90 s, 35 kg cm^{-2}) an E-TEK cathode (2.0 mg cm^{-2} Pt loading, 40% metal/C, 40% PTFE, 0.8 mg cm^{-2} Nafion) and the home made anode on a Nafion® 117 membrane.

XRD patterns were recorded using a Siemens diffractometer in the Bragg–Brentano geometry with a CuK_α X-ray radiation with about 10 mg of a powder composed of PTFE, C and Pt/Ru. The EDX measurements were performed with a Philips CM 120 microscope/EDX analyser equipped with a La B6 filament. For the transmission electron microscopy (TEM) the sample was embedded in a polymeric resin and cut into a section as small as 50 nm with an ultramicrotome. A diamond knife was used to cut the sample. The localization of the Pt and Ru by secondary electron microscopy (SEM) was determined by X-ray mapping.

The fuel cell tests in a single DMFC with a 5 cm^2 geometric surface area were carried out with a Globe Tech test bench. The E against j and P against j curves were recorded using a high power potentiostat (Wenking model HP88) interfaced with a PC to apply the current sequences and to store the data, and a variable resistance in order to fix the applied current to the cell.

3. Results and discussion

3.1. *Electrode preparation and characterization*

Several electrodes were prepared with the different compositions listed in Table 1. According to Choi et al. [28], the best conditions for preparing the most effective fuel cell cathodes by galvanostatic pulse electrodeposition of platinum at carbon were: $j = 20$ mA cm^{-2}, $t_{on} = 0.1$ s, $t_{off} = 0.3$ s. Under these conditions, Choi et al. obtained well-defined Pt particles with a distribution size around 2 nm and excellent performance in an H_2/O_2 fuel cell. Thus, our study on the anode preparation was carried out under conditions close to those of [28].

According to Cheh [29], the rate determining step of pulse electrodeposition is controlled by mass transport. Then, two different relaxation times ($t_{off} = 0.1$ s and 2.5 s) were used to determine the effect of reequilibrating the concentration of metal salts at the electrode surface on the particle size and composition. Theoretically, the

deposition of 2.0 mg cm^{-2} of metals on 10 cm^2 carbon electrodes requires 4.2, 4.4 and 4.6 C cm^{-2} for Pt/Ru catalysts with an atomic ratio of 80/20, 65/35 and 50/50, respectively. The calculation of the time necessary for metal deposition, assuming a faradaic yield of 100%, gives about 90 and 15 min, with $t_{off} = 2.5$ s and 0.3 s, respectively, and $t_{on} = 0.1$ s. However, it took several hours to obtain metal deposition at the electrode surface, indicating that the faradaic yield is very low, i.e. about 10%. Two explanations are proposed: first, the variation of the electrode potential during the current pulse leads to a nonfaradaic current due to the charge of the double layer capacity (which is important in the case of a carbon support), so that only a part of the overall applied current is involved in the electrochemical reaction [30]; secondly, as soon as some platinum particles are formed on the surface of the carbon electrode, hydrogen evolution takes place during the pulse of negative current. Both these effects are responsible for the decrease in the faradaic yield. It is then difficult to estimate the deposition time necessary for preparing electrodes containing the desired metal loading. To control the catalyst composition and loading, the concentration of metallic salts in solution was chosen to lead to a theoretical loading of 2.5 mg cm^{-2} if all the metal is deposited. In that way, the catalyst composition should be close to the ratio of the metal salt concentrations. The remaining solution was then analysed by atomic absorption spectroscopy in order to determine the amount of platinum and ruthenium which did not react and further to evaluate the loading and composition of the catalysts at the carbon electrode. Results gave catalyst loading values between 1.92 and 2.1 mg cm^{-2}, which is very close to that expected. The Pt/Ru atomic ratios listed in Table 1 indicate that the experimental values are again in good agreement with those expected.

The XRD patterns of different anodes (Figure 2) show characteristic peaks of a platinum ccp structure. It can also be seen that the diffraction peaks shift towards higher 2θ values when the Pt/Ru ratio is decreasing. The value of the lattice parameter as obtained from the refinement of the whole pattern [31] indicates that a Pt–Ru alloy was formed. Using the Williamson and Hall plot [32], the particle size of the catalysts could be evaluated. It was found to be close to $\bar{d} \approx 7$ nm and $\bar{d} \approx 5$ nm with $t_{off} = 2.5$ s and 0.3 s, respectively. It is

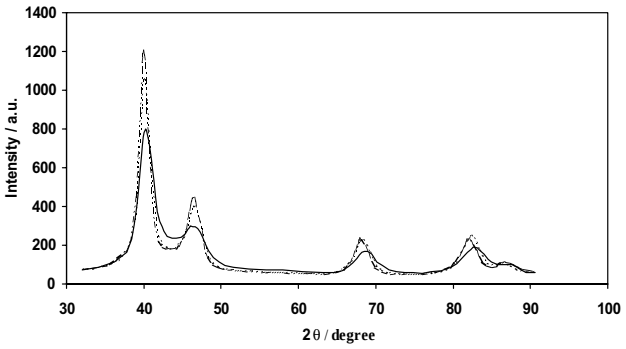

Fig. 2. XRD pattern of 80–20 (- - -); 65–35 (···) and 50–50 (—) Pt–Ru/C anodes prepared by galvanostatic pulse electrodeposition.

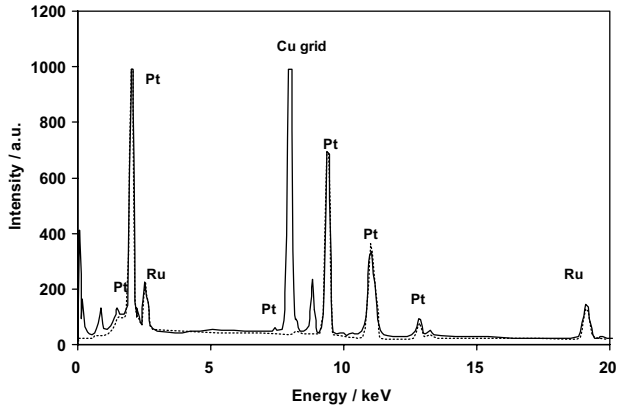

Fig. 3. EDX measurements on a 65–35 Pt–Ru/C anode.

then clear that the choice of t_{off} is very important. Applying the Vegard law for a true alloy and the values of the cell parameter for bulk alloys as determined by Vogel et al. [33], we succeeded in evaluating the atomic ratio. In Table 1, the XRD results are compared with those obtained using EDX (Figure 3) and atomic absorption spectroscopy (AAS) showing a good agreement in the analytical results.

The TEM image (Figure 4(a)) shows the formation of aggregates with sizes between 20 and 50 nm. These aggregates are in fact comprised of smaller particles as shown in Figure 4(b). The average size of the particles is close to 8 and 5 nm for $t_{off} = 2.5$ s and $t_{off} = 0.3$ s, respectively, in good agreement with the XRD results. These particle sizes are rather greater than those

Table 1. Electrodes preparation and characterization

Electrode	Pt/Ru atomic ratio in solution	t_{off} /s	Atomic ratio			Particle size /nm
			XRD	EDX	AAS	
PtRu 50–50	50/50	2.5	55/45	60/40	–	~7–8
PtRu 50–50	50/50	0.3	57/43	53/47	48/52	~5
PtRu 65–35	65/35	2.5	69/31	69/31	–	~7–8
PtRu 65–35	65/35	0.3	66/34	–	69/31	~5
PtRu 80–20	80/20	2.5	75/25	82/18	–	~7–8
PtRu 80–20	80/20	0.3	77/23	78/22	78/22	~5

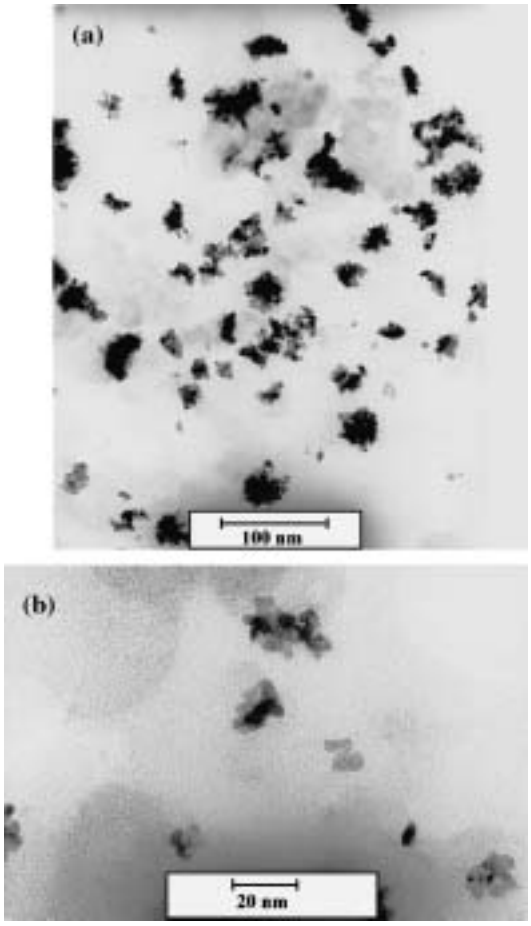

Fig. 4. TEM photographs of 65–35 Pt–Ru/C catalyst from an anode prepared by galvanostatic pulse electrodeposition with $t_{off} = 2.5$ s. Scale: (a) 100 nm, (b) 20 nm.

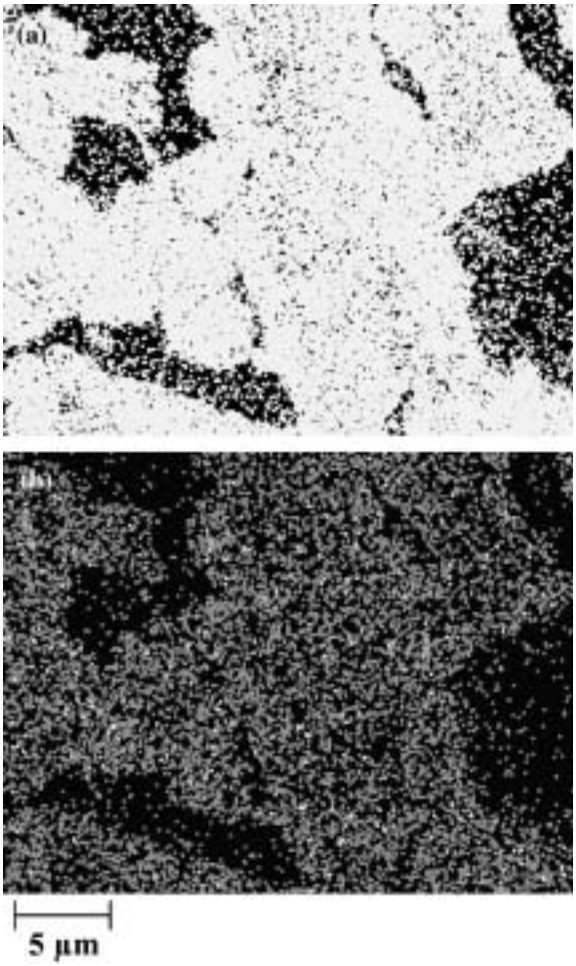

Fig. 5. Secondary electron microscopy (SEM) of a 65–35 Pt–Ru/C catalyst from an anode prepared by galvanostatic pulse electrodeposition with $t_{off} = 2.5$ s. (a) Pt L_α, (b) Ru K_α.

obtained by Choi et al. [28], indicating that the nucleation or growth mechanism is different with Pt/Ru than with Pt. In spite of this, the bigger size of our particles is not necessary bad for methanol oxidation, since Frelink et al. [34] showed that the best specific activity for methanol oxidation on a Pt/C catalyst was obtained with particle sizes greater than 4.5 nm.

Secondary electron microscopy (SEM) was used to determine the spatial repartition of platinum (Figure 5(a)) and ruthenium (Figure 5(b)). Both these metals are located in the same place on the electrode surface. This result can be correlated with the data obtained from XRD which indicate that the metallic phase is mainly an alloy of platinum and ruthenium.

3.2. *Fuel cell tests*

The electrodes were tested in a single 5 cm^2 surface area DMFC in order to determine their electrochemical behaviour under operating conditions. Figure 6 shows the performances of a 80–20 Pt–Ru/C anode as a function of temperature. Increasing the temperature leads to improved performance. The maximum power density at 50 °C, close to 12 mW cm^{-2}, is greatly enhanced (about ten times higher) when the temperature

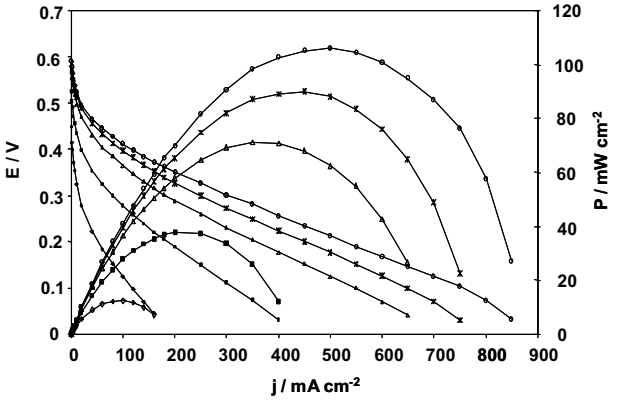

Fig. 6. Cell voltage (E) and power density (P) against current density (j) in a single 5 cm^2 surface area DMFC with a 80–20 Pt–Ru/C anode prepared with $t_{off} = 0.3$ s, at different temperatures (Nafion® 117 membrane, 2 M CH_3OH). Temperature: (◇) 50, (■) 70, (△) 90, (*) 100 and (○) 110 °C.

reaches 110 °C. This fact confirms the difficulty of oxidizing methanol and the necessity to work at temperatures higher than 100 °C to enhance the electrode kinetics, and thus, the DMFC performance.

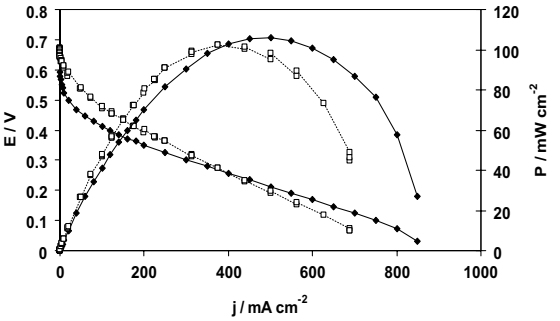

Fig. 7. Cell voltage (E) and power density (P) against current density (j) in a single 5 cm^2 surface area DMFC with a 80–20 Pt–Ru/C anode prepared with $t_{off} = 0.3$ s (♦) and commercial E-TEK anode 50–50 (□), at 110 °C (Nafion® 117 membrane, 2 M CH_3OH, $P_{O_2} = 2.5$ bar; $P_{MeOH} = 2.0$ bar).

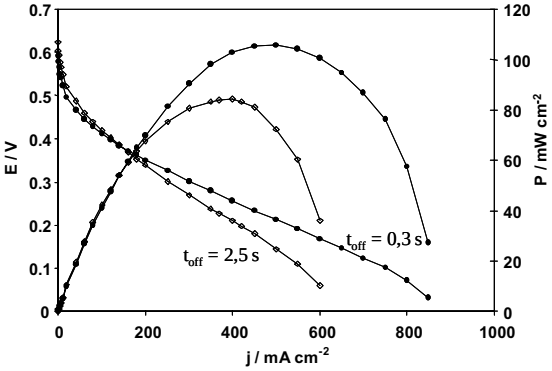

Fig. 8. Cell voltage (E) and power density (P) against current density (j) in a single 5 cm^2 DMFC with a 80–20 Pt–Ru/C anode prepared with $t_{off} = 0.3$ s (●) and $t_{off} = 2.5$ s (◇) at 110 °C (Nafion® 117 membrane, 2 M CH_3OH, $P_{O_2} = 2.5$ bar; $P_{MeOH} = 2.0$ bar).

Comparison of the 80–20 Pt–Ru/C anode with a commercial 50–50 Pt–Ru/C anode from E-TEK (Figure 7) shows that the former electrode gives best performance in term of power density, the maximum of power density being close to 100 mW cm^{-2} with the E-TEK anode and to 110 mW cm^{-2} with the 80–20 Pt–Ru/C anode. Power density values of 100 mW cm^{-2} achieved with E-TEK catalysts are rather low when compared with data of Shukla et al. [35]. These authors achieved 180 mW cm^{-2} at 90 °C under ambient pressure of oxygen. But, they used cathodes with a 4.6 mg cm^{-2} platinum loading which minimizes the methanol cross-over effect and likely enhances the cathode efficiency. In our experiments, all parameters being kept constant, comparison between the commercial and home made anodes is consistent. For lower current densities, the commercial anode displays the best performance whereas higher current densities are achieved with the home made anode. This difference can be explained by catalyst composition of the anode which is 50/50 for the commercial anode and 80/20 for the home made anode. In addition, the PTFE loading in the commercial anode is twice higher than that in the home made anode (i.e., 30 and 15 wt.%, respectively). The PTFE being hydrophobic, the diffusion of the methanol/water mixture towards the catalytic sites is easier with a low PTFE loading, lowering the mass transfer limitation and then increasing the performance at high current densities.

In Figure 8, the importance of t_{off} is clearly demonstrated. Best performance in terms of maximum power density was obtained with $t_{off} = 0.3$ s, as claimed by Choi et al. [28]. This fact can be correlated with the size distribution of the catalyst particles, as determined by EDX and XRD. Indeed, the particle sizes are smaller and better distributed with $t_{off} = 0.3$ s than with $t_{off} = 2.5$ s. It is also clear from Figure 9(a) and (b) that, in the temperature range 50 to 110 °C, the best performance in terms of maximum power density is obtained with a Pt/Ru atomic ratio of 80/20, whatever the conditions used for the preparation of the anodes. This result confirms those already obtained in a classical three-electrode electrochemical cell [36]. Indeed, the

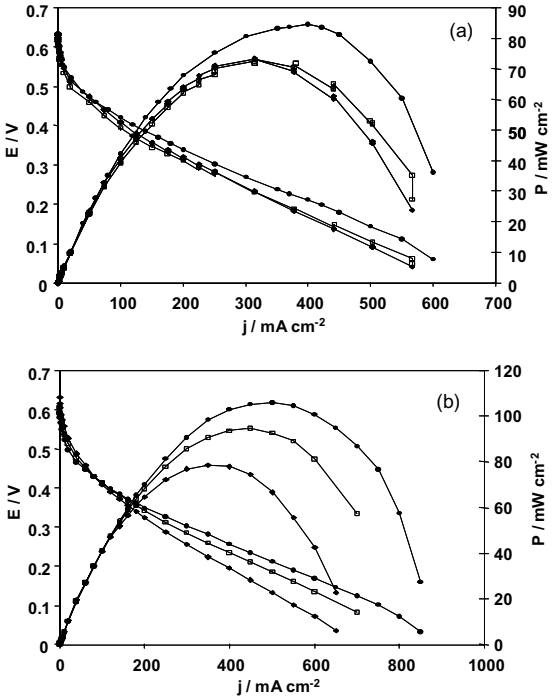

Fig. 9. Cell voltage (E) and power density (P) against current density (j) in a single 5 cm^2 surface area DMFC with different Pt–Ru/C anodes, at 110 °C (Nafion® 117 membrane, 2 M CH_3OH, $P_{O_2} = 2.5$ bar, $P_{MeOH} = 2.0$ bar). Key: (♦) Pt–Ru: 50–50; (□) Pt–Ru: 65–35; (●) Pt–Ru: 80–20. (a) $t_{off} = 2.5$ s; (b) $t_{off} = 0.3$ s.

model of methanol electrooxidation involves four platinum sites for the dissociative adsorption of methanol and one ruthenium site for the water molecule activation as shown by *in situ* FTIR spectroscopic studies [37]. Other authors [38–40] also claimed that the best platinum/ruthenium atomic ratio for methanol oxidation was between 20 and 30%. But it is possible that increasing the temperature involves some changes in the oxidation mechanism of methanol and then in the optimal Pt/Ru atomic ratio. Thermal activation of ruthenium may give it the ability to adsorb and dehydrogenate methanol at temperatures greater than 40 °C [41].

4. Conclusions

The main goal of this study was to prepare reproducibly new Pt–Ru bimetallic electrocatalysts by galvanostatic pulse electrodeposition. We obtained interesting results concerning the anode preparation and the behaviour of these anodes in a DMFC that can be summarised as follows:

(i) The galvanostatic pulse electrodeposition method is convenient in terms of controlling the catalyst loading and composition (atomic ratio).
(ii) The catalysts show an alloy character as determined by XRD.
(iii) The performance in a DMFC of such new bimetallic electrodes are better than that obtained with a commercial E-TEK anode.
(iv) In the temperature range used to carry out this study, the best platinum/ruthenium atomic ratio is close to 80/20.
(v) The influence of t_{off} on the structure and performance of the electrodes is crucial.

Although the faradaic yield is low, this method of preparing supported catalysts on a high surface area carbon electrode is very convenient for industrial application: no organic solvent is required, the deposition by consumption of the metal salts in solution allows control of the metal loading on the electrode and the same batch can be reused by adding metal salts and sulfuric acid to adjust the concentrations. Moreover, by varying different parameters (t_{on}, t_{off}, concentration of metallic salts, pulse current density, etc.), the structure and nature of the bimetallic catalyst can be changed and adapted to the desired application.

Acknowledgement

This work was carried out under the framework of the Commission of the European Union through the NEMECEL program (Joule III, JOE3-CT97-0063).

References

1. C. Lamy, J-M. Léger and S. Srinivasan, *in* J.O'M. Bockris, B.E. Conway and R.E. White (Eds), 'Modern Aspects of Electrochemistry', vol. 34, (Kluwer Academic/Plenum, New York, 2001), chapter 3, pp. 53–118.
2. B. Höhlein, P. Biedermann, T. Grube and R. Menzer, *J. Power Sources* **84** (1999) 203.
3. C. Coutanceau, M-J. Croissant, T. Napporn and C. Lamy, *Electrochim. Acta* **46** (2000) 579.
4. S. Motoo, M. Watanabe and N. Furuya, *J. Electroanal. Chem.* **160** (1984) 351.
5. M.S. Wilson and S. Gottesfeld, *J. Appl. Electrochem.* **22** (1992) 1.
6. A.K. Shukla, P.A. Christensen, A.J. Dickinson and A. Hamnett, *J. Power Sources* **76** (1998) 54.
7. S.C. Thomas, X. Ren and S. Gottesfeld, *J. Electrochem. Soc.* **146** (1999) 4354.
8. P. Argyropoulos, K. Scott and W.M. Taama, *J. Power Sources* **87** (2000) 152.
9. A. Fisher, J. Jindra and H. Wendt, *J. Appl. Electrochem.* **28** (1998) 277.
10. P.L. Antonucci, A.S. Arico, P. Creti, E. Ramunni and V. Antonucci, *Solid State Ionics* **125** (1999) 431.
11. T.J. Schmidt, M. Noeske, H.A. Gasteiger, R.J. Behm, P. Britz and H. Bönnemann, *J. Electrochem. Soc.* **145** (1998) 925.
12. T.J. Schmidt, M. Noeske, H.A. Gasteiger, R.J. Behm, P. Britz, W. Brijoux and H. Bönnemann, *Langmuir* **13** (1997) 2591.
13. S. Mukerjee, *J. Appl. Electrochem.* **20** (1990) 537.
14. A. Lima, C. Coutanceau, J-M. Léger and C. Lamy, *J. Appl. Electrochem.* **31** (2001) 379.
15. W.T. Napporn, J-M. Léger and C. Lamy, *J. Electroanal. Chem.* **404** (1996) 153.
16. X. Ren, M.S. Wilson and S. Gottesfeld, *J. Electrochem. Soc.* **143** (1996) L12A.
17. S. Wasmus and W. Vielstich, *J. Appl. Electrochem.* **23** (1993) 120.
18. P. Waszczuk, A. Wieckowski, P. Zelenay, S. Gottesfeld, C. Coutanceau, J-M. Léger and C. Lamy, *J. Electroanal. Chem.* **511** (2001) 55.
19. N.P. Leisner, C.B. Nielsen, P.T. Tang, T.C. Dörge and P. Moller, *J. Mater. Process. Techn.* **58** (1996) 39 and references therein.
20. C. Catteneo, M.I. Sanchez de Pinto, H. Mishima, B.A. Lopez de Mishima and D. Lescano, *J. Electroanal. Chem.* **461** (1999) 32.
21. E.J. Taylor, E.B. Anderson and N.R. Vilambi, *J. Electrochem. Soc.* **139** (1992) 145.
22. T. Napporn, M-J. Croissant, J-M. Léger and C. Lamy, *Electrochim. Acta* **43** (1998) 2447.
23. A.D. Jannakoudakis, E. Theodoridou and D. Jannakoudakis, *Synth. Met.* **10** (1984/85) 131.
24. D-L. Lu and K-I. Tanaka, *Surf. Sci.* **373** (1997) L339.
25. A.A. Mikhaylova, O.A. Khazova and V.S. Bagotzky, *J. Electroanal. Chem.* **480** (2000) 225.
26. F. Gloaguen, J-M. Léger, C. Lamy, A. Marmann, U. Stimming and R. Vogel, *Electrochim. Acta* **44** (1999) 1805.
27. S.D. Thomson, L.R. Jordan and M. Forsyth, *Electrochim. Acta* **46** (2001) 1657.
28. K.H. Choi, H.S. Kim and T.H. Lee, *J. Power Sources* **75** (1998) 230.
29. H.Y. Cheh, *J. Electrochem. Soc.* **118** (1971) 1132.
30. A.J. Bard and L.R. Faulkner, 'Electrochemical Methods: Fundamentals and Applications' (J. Wiley & Sons, New York, 1980), p. 258.
31. W. Kraus and G. Nolze, 'CPD International Union of Crystallography', Newsletter No. 20 (1998).
32. G.K. Williamson and W.H. Hall, *Acta Metall.* **1** (1953) 22.
33. W. Vogel, P. Britz, H. Bönnemann, J. Rothe and J. Hormes, *J. Phys. Chem. B* **101** (1997) 11029.
34. T. Frelink, W. Visscher and J.A.R. Veen, *J. Electroanal. Chem.* **382** (1995) 65.
35. A.K. Shukla, C.L. Jackson, K. Scott and R.K. Raman, *Electrochim. Acta* **47** (2002) 3401.
36. L. Dubau, C. Coutanceau, E. Garnier, J-M. Léger and C. Lamy, *J. Appl. Electrochem.* (2003), in press.
37. A. Kabbabi, R. Faure, R. Durand, B. Beden, F. Hahn, J-M. Léger and C. Lamy, *J. Electroanal. Chem.* **444** (1998) 41.
38. R. Ianiello, V.M. Schmidt, U. Stimming, J. Stumper and A. Wallau, *Electrochim. Acta* **39** (1994) 1863.
39. V.S. Entina and O.A. Petrii, *Sov. Electrochem.* **4** (1968) 97.
40. T. Iwasita, H. Hoster, A. John-Anaker, W.F. Lin and W. Vielstich, *Langmuir* **16** (2000) 522.
41. D. Chu and S. Gilman, *J. Electrochem. Soc.* **143** (1996) 5.